

DOWNHOLE ELECTRODYNAMIC HEATER PROJECT FOR THE PERMEABILITY MAGNIFICATION OF HIGH-VISCOSITY OIL BED

Ponomarenko A.G, Buyanov G.O, Ruhman A.A, Shikanov A.E., Shikanov E.A., Bannikov R.V., Sevastianov A.V.

1. INTRODUCTION

The work [1] provides information on the structure of proven oil reserves in Russia. It shows that the share of heavy oils in the overall reserves makes up a large proportion, roughly 40%. Currently conventional (light) oil accounts for the bulk of oil production. The well-bottom zone (WBZ) with heavy oil has low permeability and special oil recovery methods should be implemented [2]. These could include treatment of WBZ with chemical reagents, hydraulic fracturing treatment, methods for WBZ treatment with intensive acoustic waves, thermal stimulation by heated steam or liquid and so on. These technologies have a number of shortcomings. For example, a long period of time to perform technological activities, high work costs, difficulties in obtaining conditions necessary for environmental safety, high energy consumption. This paper presents a new method of oil viscosity reduction by means of local induction heating.

2. OPERATING PRINCIPLE OF A DOWNHOLE ELECTROMAGNETIC HEATER

A downhole electromagnetic induction heater implements a technical solution [3,4] protected by a patent of the Russian Federation. In the simplest case, it represents a multi-turn solenoid powered by the RF current (about 10 kHz) and positioned coaxially within the casing pipe.

The heating system could be described as a coaxial transformer with single-turn secondary winding, the role of which is played by the casing. Being excited in the casing, an azimuthally directed alternating current with the density $j(r)$ due to the "skin-effect" [5] will accumulate in a narrow layer of thickness δ (see Fig. 1).

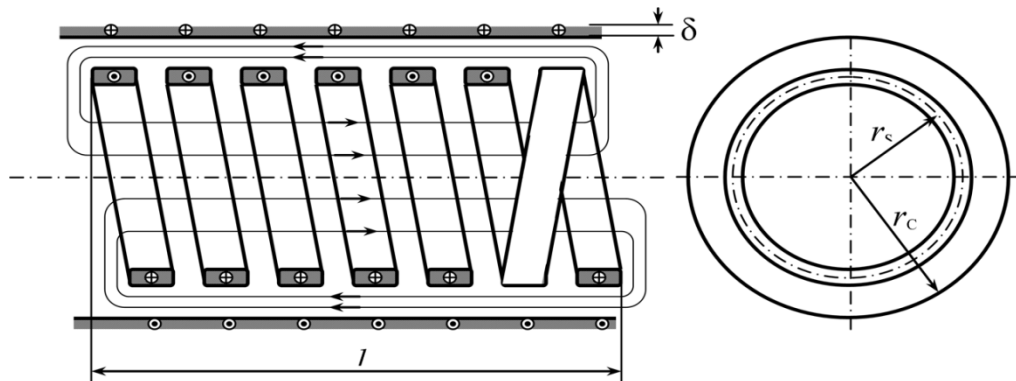


Fig. 1. The induction heater. l - length of the solenoid, r_s, r_c - radii of the solenoid and the casing respectively

The power released by the current flowing is defined by the expression:

$$P = \rho \int_V dV j(\mathbf{r})^2 \approx 2\pi\rho \frac{I^2 r_c}{l\delta} = \frac{2I^2 r_c}{l} \sqrt{\pi^3 \mu_0 \mu_c \rho f} = \frac{I^2 R_c}{2}, \tag{1}$$

where V is the volume, which contains an induction current, I is the current flowing in it, ρ is the resistivity of the casing material, μ_c is the relative magnetic permeability of steel which the casing is made of, $\mu_0 = 4\pi \cdot 10^{-7} \text{ Hn/m}$ - the magnetic constant, R_c is the effective electric resistance of the casing.

The power released is partially transferring through the cement column into a formation and heating it.

3. ELECTRODYNAMIC CALCULATION OF THE OPERATING VERSION OF A DOWNHOLE ELECTROMAGNETIC HEATER

The mentioned above diagram of a downhole induction heater for heating the casing is an idealized version and cannot serve as the basis for developing an operating device due to poor efficiency related to magnetic flux leakage. In order to minimize the flux leakage, it was suggested that a cylindrical ferrite shield with relative magnetic permeability μ_f should be mounted inside the solenoid, as shown in Fig. 2.

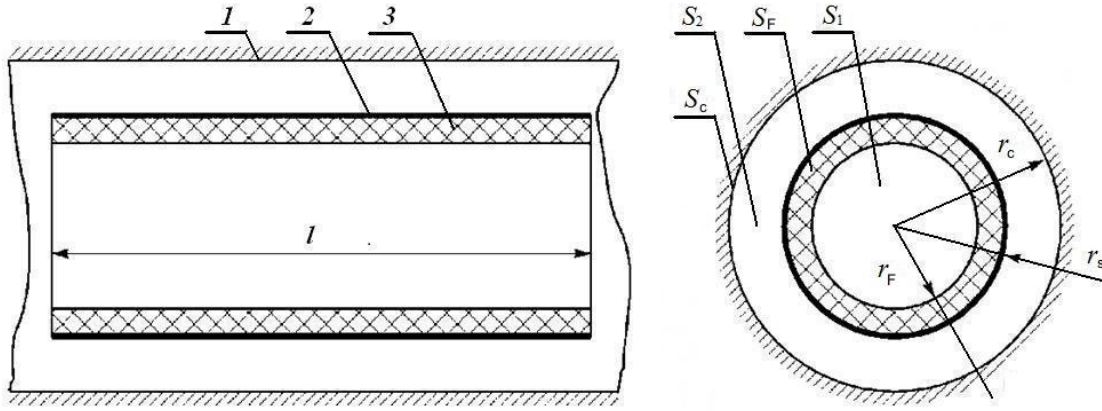


Fig. 2. Inductor with ferrite: 1 – casing pipe, 2 – one-layer winding, 3 – ferrite

The law of magnetic flux continuity states that the sum of fluxes Φ_1 and Φ_F , which penetrate internal cross sections: a cross section S_1 covered with a ferrite shield and a cross section of a ferrite shield S_F , is equal to the sum of fluxes Φ_2 and Φ_C , which penetrate external cross sections S_2 and space inside the casing:

$$\Phi_1 = B_1 S_1, \quad \Phi_F = B_F S_F, \quad \Phi_2 = B_2 S_2, \quad \Phi_C \approx 2\pi B_C r_C \delta, \quad (4)$$

where

$$B_1 = \mu_0 H_1, \quad B_2 = \mu_0 H_2, \quad B_F = \mu_F \mu_0 H_1, \quad B_C \approx \mu_C \mu_0 H_2, \quad (5)$$

H_1 and H_2 are the amplitudes of the magnetic field strengths inside and outside the solenoid. The latter two formulae in (4) and (5) assume that the fields are averaged over a radius, taking into account their exponential decay in accordance with the “skin-effect” theory [5]. From the condition of continuity of the total magnetic flux -

$$\Phi_1 + \Phi_F = \Phi_2 + \Phi_C,$$

taking into account the ratios (4) and (5) we have the following relationship between the magnetic field strengths inside and outside the solenoid:

$$H_1 = \frac{S_2 + 2\pi\mu_C r_C \delta}{S_1 + \mu_F S_F} H_2 = \frac{r_C^2 - r_S^2 + 2\mu_C r_C \delta}{r_F^2 + \mu_F (r_S^2 - r_F^2)} H_2 \quad (6)$$

By neglecting magnetic leakage fields, the Ampere’s law implies the following ratio:

$$nI_1 \approx (H_1 + H_2)l,$$

where n is the number of solenoid turns, I_1 is the current flowing through the solenoid circuit. From this formula, taking into account (6), we have the relationship between the magnetic field strength at the surface of the casing and the current I_1 :

$$H_2 \approx \frac{na}{l} I_1, \quad (7)$$

$$a = \frac{r_S^2 + \mu_F (r_S^2 - r_F^2)}{r_C^2 + (\mu_F - 1)(r_S^2 - r_F^2) + 2\mu_C r_C \delta}$$

where

The dimensionless structural parameter a determines the degree of the magnetic field strength near the casing wall without increasing the current or the number or solenoid turns, but only by using a ferrite shield and the ratio between radii of the casing and of the solenoid. To take into account the effect of these factors, it should be considered as a function from the thickness of a ferrite shield to the radius of the solenoid. Fig.3 shows a calculated set of such dependencies.

The Ampere’s law also implies the relation of a current excited in the casing to the magnetic field strength at its surface:

$$I \approx lH_2. \quad (8)$$

Fig. 4 shows a cross section fragment of the casing with the solenoid inside it and diagrams of induction (the middle diagram) and of the magnetic field strength (the bottom diagram) taking into account the averaging over the casing cross section. Again, we assume that the magnetic field configuration corresponds to the pattern in Fig.1 and do not take into account the spatial decay of its strength at the ends of a coil. The accurate computer calculations showed that in the engineering calculations such an assumption does not lead to significant errors (deviations not exceeding 10%).

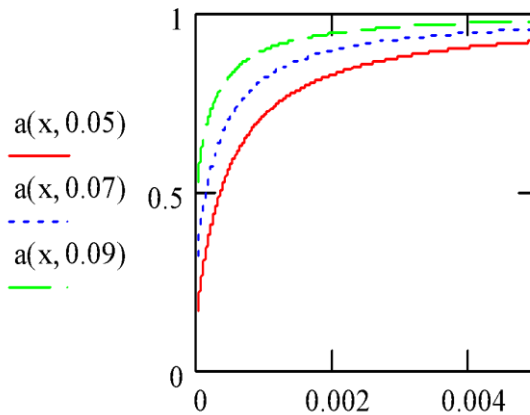


Fig. 3. Set of dependencies $a(x, rS)$

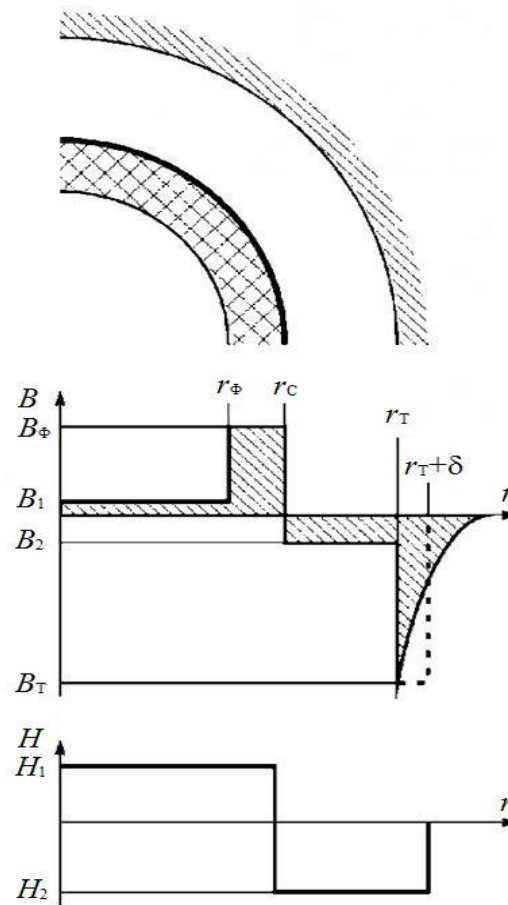


Fig. 4. Diagrams of magnetic induction amplitudes and the magnetic field strength across the cross section of the casing with an inductor

4. THE EQUIVALENT RESISTANCE AND INDUCTANCE OF AN INDUCTOR

By neglecting resistive losses in the solenoid, we have from the equation for power:

$$P \approx \frac{R_c I^2}{2} \approx \frac{R I_1^2}{2},$$

taking into account (1), (3), (7) and (8), the expression for the equivalent resistance of the inductor electric circuit:

$$R \approx n^2 a^2 R_C = \frac{4\pi n^2 \rho a^2 r_C}{l \delta} = \frac{4n^2 a^2 r_C}{l} \sqrt{\pi^3 \rho f \mu_C \mu_0} \quad (9)$$

To determine the heater inductance the ratio between total magnetic flux and the coil current should be evaluated. Formulae (4), (6) and (7) imply the following ratio:

$$\Phi_1 + \Phi_F = \Phi_2 + \Phi_C = \frac{\mu_0 n a}{l} (S_2 + 2\mu_C \pi r_C \delta) I_1$$

This expression by definition of [5] implies the desired formula for the heater equivalent inductance.

$$L = \frac{\Phi_2 + \Phi_C}{I_1} = \frac{\pi \mu_0 n a}{l} (r_C^2 - r_s^2 + 2\mu_C r_C \delta) \quad (10)$$

5. EXPERIMENTAL TESTS OF AN INDUCTOR

In order to verify the presented electrodynamic model, the following experiment with the solenoid was conducted. The solenoid dimensions was $S=0.02\text{m}$, $l=0.084\text{m}$, it contained 60 turns of copper wire. The solenoid was placed into the steel pipe ($\mu_C=400$ $\mu\rho=7 \cdot 10^{-8}$ Ohm·m) with internal diameter of 0.05m and interconnected into the electrical circuit as shown at fig.5.

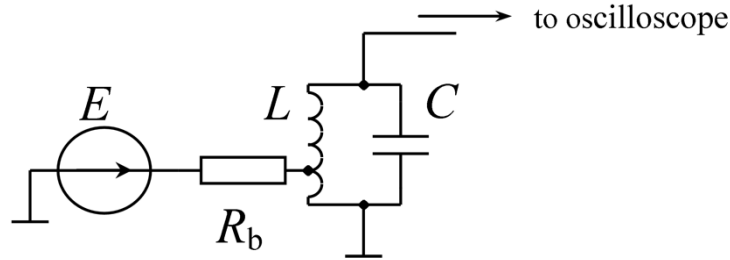


Fig5. Scheme set up for measuring the equivalent resistance and inductance of the heater's inductor. E- RF voltage source, Rb- voltage source output resistance, L- solenoid inductance, C- resonant capacitor.

During the measurements, the resonance frequency f_0 and the Q of the circuit were determined. The equivalent inductance and resistance of the heater were calculated using the formulas:

$$L = \frac{1}{4\pi^2 f_0^2 C} \quad R = \frac{1}{Q} \sqrt{\frac{L}{C}}$$

The table 1 shows the results of a comparison of theoretical, calculated by formulae (9) and (10), and experimental values.

Table 1

f0, Hz	R, Ohm	Rexp, Ohm	L, μH	Lexp, μH
11640	0.845	0.840	45,5	46.7
24800	1.73	1.60	41.2	41.3

As could be seen in table 1 the experimental and previously calculated values of R and L are in good correspondence to each other. These tests of experiments like for different pipe diameters was conducted. This allows us to use the developed math during designing of the fully functional induction heater.

6. LABORATORY TESTING OF THE INDUCTION HEATER OPERATION

As the result of studies conducted the fully operational induction heater demonstration unit was designed and assembled. The appearance of the assembled coil with single layer winding is presented on Fig. 6.



Fig. 6. The induction heater coil appearance.

As a part of the operational testing, the thermal experiment with heating of a section of steel pipe was carried out. Parameters of the pipe used: height $H = 1.3\text{m}$, inner radius $r_c = 0.05\text{m}$, wall thickness $h = 0.004\text{m}$ (Fig. 7).

During the thermal experiment local temperature on the outer surface of the pipe rose from 20°C to 60°C in 30 seconds. Taking into consideration the metal volume and heat transfer the total heating power of nearly 1kW is estimated. At the moment our team is working on high-power variant with expected heating power of 3kW . The estimations show that such power could be enough to locally heat the casing pipe to the temperature under which the oil viscosity would significantly (potentially by an order of magnitude) reduce.



Fig. 7. "Submerging" of the heater coil into the casing pipe equivalent

7. FORMATION OF THE TEMPERATURE FIELD IN THE WELL

The heating process is conducted by repetitive sliding of the heater coil up and down through the heating area of the casing pipe on length L . The heat is partially transferred to the WBZ and creates temperature field $T(r, z, t)$ in the formation. To estimate that temperature field the following differential heat equation [6] could be used:

$$\frac{\partial \theta}{\partial t} \approx a^2 \Delta \theta + \frac{P_0 \Pi(z + \frac{L}{2}) \Pi(\frac{L}{2} - z)}{4\pi c \rho \delta(f) L r_T}, \quad (11)$$

where $\theta(r, z, t) = T(r, z, t) - T_0$ - increment of the temperature to the time t in the point with cylindrical coordinates r, z ,

$$a = \sqrt{\frac{\lambda}{c\rho}}$$

T_0 - initial temperature, ρ, c, λ , - respectively, density, specific heat and thermal conductivity of the heated medium, $\Pi(x)$ - Heaviside step function. The solution of equation (11) gives an expression for the temperature field:

$$\theta(r, z, t) = \frac{P_0}{8\pi^2 L \lambda} \int_{-\frac{L}{2}}^{\frac{L}{2}} d\xi \int_0^\pi d\varphi \frac{1 - \operatorname{erf}\left\{ \frac{R[r, r_T, (z - \xi), \varphi] \sqrt{c\rho}}{2\sqrt{\lambda t}} \right\}}{R[r, r_T, (z - \xi), \varphi]}$$

where $R[r, r_T, (z - \xi), \varphi] = \sqrt{r^2 + r_T^2 - 2rr_T \cos \varphi + (z - \xi)^2}$

Fig.8 shows the calculated distribution of the temperature field.

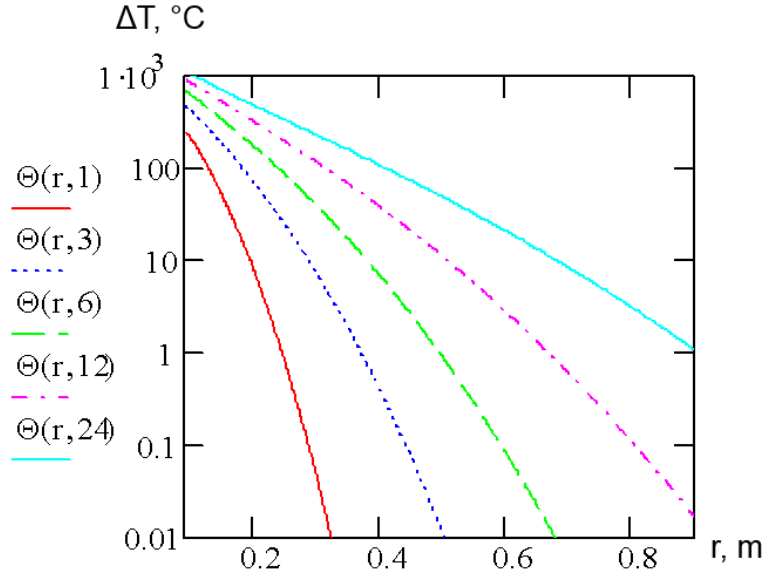


Fig.8. Calculated distribution of the temperature field $\Theta(r,t)$ on $z=0$. Time scalet is in hours.

8. REDUCTION OF THE HEAVY OIL VISCOSITY COEFFICIENT BY USING AN INDUCTION HEATER

In order to understand the requirements for the casing pipe induction heater, we analyzed the experimental dependencies of the oil viscosity coefficient on temperature. The example of data from the work [7] shows that they can be approximated by a decaying exponential curve with amplitude A and the temperature decrement in the form B :

$$\eta(\theta) \cong B \exp(-A\theta) \quad (11)$$

To find the parameters A and B by experimental data it is possible to use the method of least squares, the implementation of which is reduced to the solution of the following system of equations:

$$\begin{cases} \ln B + A \sum_{k=1}^K t_k^2 = \sum_{k=1}^K t_k \ln \eta_k \\ \ln B + A \sum_{k=1}^K t_k = \sum_{k=1}^K \ln \eta_k \end{cases}$$

where η_k is the experimental values of the viscosity coefficient at $\theta = \theta_k$, K - the number of experimental points.

This dependence is in accordance with the exponential model of liquid viscosity. With its use, the spatial and time dependences of the viscosity coefficient for a particular well were calculated, shown in fig.9.

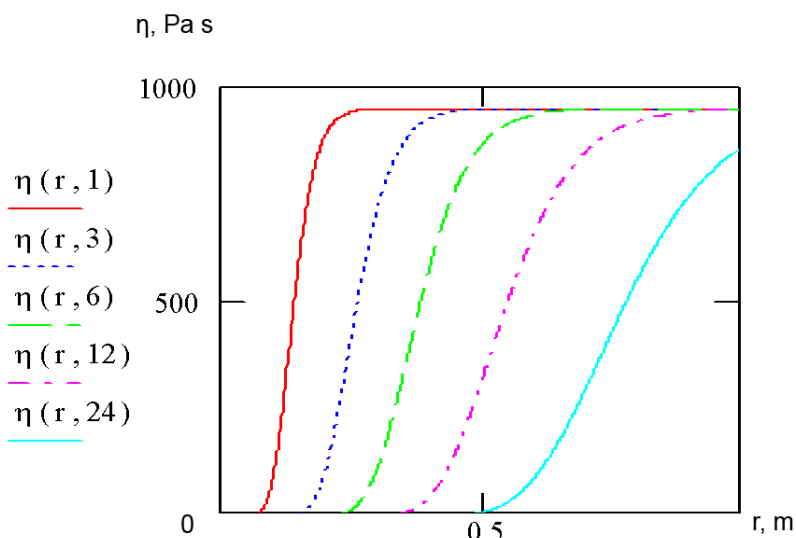


Fig.9. Specific spatial and temporal dependence $\eta(r,t)$ of the viscosity ratio. Time scale is in hours.

The analysis of this dependence suggests that it is possible to develop a downhole RF generator with a frequency of ~ 10 kHz and a power sufficient to reduce the viscosity coefficient of oil difficult to extract to the values of the viscosity coefficient of conventional oils.

9. CONCLUSIONS

1. To summarize the above data, it can be stated that the proposed project for a downhole induction heater of the reservoir with high-viscosity oil allows local heating of the oil formation in the area of WBZ.
2. The performed calculations demonstrated possibility for a substantial reduction (more than 10 times) of the oil viscosity coefficient in the formation areas close to the casing.
3. The work was performed as a part of Russian Science Foundation Grant Agreement №15-19-00151 to conduct fundamental and pilot studies.

10. REFERENCES

- [1] Antoniadis D.G. et al. Oil production status by enhanced recovery methods in the total volume of world production. Neftyanoe hozyajstvo [Oil industry], №1, 1999, pp. 16-23, (in Russian).
- [2] Ibragimov L.K., Mischenko I.T., Chelobjants D.K. Intensifikaciya dobychi nefi [Oil production intensification], Moscow, Nauka Publ, 2000, 414 p. (in Russian).
- [3] Bogdanovich B.Yu., Dmitriev M.S., Ilyinsky A.V., et al. Patent RU168526U1, application filed 29.07.2016.
- [4] Bogdanovich B.Yu., Ilyinsky A.V., Nesterovich A.V. et al. Patent RU2631451C1, application filed 29.07.2016.
- [5] Landau L.D., Livshits E.M. Elektrodinamika sploshnyh sred [Electrodynamics of continuous media]. Moscow, Nauka Publ, 1982, p.624, (in Russian).
- [6] Landau L.D., Livshits E.M. Gidrodinamika [Hydrodynamics]. Moscow, Nauka Publ, 1988, p.736, (in Russian).
- [7] Khisamov R.S., Khusin R.R., Andreev B.E., Dubinsky G.S., Mijassarov A.Sh. Perspectives for increasing the efficiency in high-viscosity oil reservoir development using energy serving technologies. Neftyanoe hozyajstvo [Oil industry], №4, 2015, pp. 54-55, (in Russian).